NANO LETTERS

2007
Vol. 7, No. 4
914−920

Systematic Investigation of the Thermodynamics of HSA Adsorption to *N-iso*-Propylacrylamide/*N-tert*-Butylacrylamide Copolymer Nanoparticles. Effects of Particle Size and Hydrophobicity

Stina Lindman,[†] Iseult Lynch,[†,‡] Eva Thulin,[†] Hanna Nilsson,[†] Kenneth A. Dawson,[‡] and Sara Linse*[,†,‡,§]

Department of Biophysical Chemistry, Chemical Centre, Lund University, P.O. Box 124, SE-221 00 Lund, Sweden, School of Chemistry and Chemical Biology, and Conway Institute, University College Dublin, Belfield, Dublin 4, Ireland

Received November 23, 2006; Revised Manuscript Received February 10, 2007

ABSTRACT

Nanoparticles in biological fluids almost invariably become coated with proteins that may confer nanomedical and nanotoxicological effects. Understanding these effects requires quantitative measurements using simple systems. Adsorption of HSA to copolymer nanoparticles of varying hydrophobicity and curvature was studied using ITC, yielding stoichiometry, affinity, and enthalpy changes upon binding. The hydrophobicity was controlled via the co-monomer ratio, *N-iso*-propylacrylamide/*N-tert*-butylacrylamide. The most hydrophobic particles become fully covered with a single layer of protein, except at high curvature.

The use of nanoparticles has grown rapidly over the last couple of years, and the number of products containing nanoparticles is increasing dramatically, including in medicine[1,2] where there are great hopes that a new era of nanomedicine will arise. Despite this rapid increase, surprisingly little is known about the responses of biological systems to these particles, and there are few overall conceptual frameworks.[3] Nanomaterials that enter the body become coated with proteins, and this may have severe effects on the protein function and conformation.[4−6] On the particle surface, there will also be an increase in the local concentrations of certain proteins, which in turn might result in attenuation or amplification of activity, protein aggregation, or disruptions of other kinds. For example, the proteins might become partially unfolded upon adsorption, producing an immune response or increasing the risk for protein misfolding diseases. For examples of conformational changes undergone by proteins upon adsorption, see refs 3, 4, and 6.

Of concern for nanobiology and nanomedicine are the potential toxicological effects of nanomaterials, and studies suggesting that nanoparticles may be toxic are beginning to emerge.[7,8] However, as with the earlier field of gene delivery, where results were greatly hampered by system irreproducibilities such as particle aggregation with time, many of the studies involving nanoparticle toxicity are somewhat ambiguous.[9] The discrepancies arise from, for example, impurities from the synthesis process remaining in the samples and generally poorly characterized, polydisperse samples whose behavior in physiological solution is not understood. Since nanoparticles are invariantly coated with proteins *in vivo*, cells or tissues never encounter the naked particles. Rather, beneficial or harmful biological effects will be mediated by the adsorbed proteins and the structure/function they take on in the particle-adsorbed state. A deep understanding of potential toxic effects will require a detailed description of the binding of proteins to nanoparticles in terms of affinities, stoichiometries, and the underlying driving forces. Each of these parameters is likely to be strongly dependent on both the particle and protein identity, as well as on the solution conditions. In order to distinguish

* Corresponding author. E-mail: Sara.Linse@bpc.lu.se or sara@fiachra.ucd.ie.
[†] Lund University.
[‡] School of Chemistry and Chemical Biology, University College Dublin.
[§] Conway Institute, University College Dublin.

10.1021/nl062743+ CCC: $37.00 © 2007 American Chemical Society
Published on Web 03/03/2007

between different effects and to pinpoint their molecular origins, there is a need for accurate and reproducible methods and simplified *in vitro* model systems that can qualitatively and quantitatively define nanoparticle−protein interactions and characterize the nanoparticle−protein complex. Recently developed methods for investigating the exchange rates of different plasma proteins upon adsorption to particles[10] reveal a large variation in exchange rates for different particle−protein combinations. In another study, plasma proteins that adsorbed to polymeric particles were identified and the relative amounts were determined.[11] These results show that it is not necessarily the most abundant proteins that dominate on the particles, but rather some of the less abundant proteins with higher affinity may become enriched on the particles. The implications of this for nanomedicine are profound.

Here we present an *in vitro* system for detailed and systematic analysis of the adsorption of an abundant serum protein to model copolymer particles of varying size and hydrophobicity. We use isothermal titration calorimetry (ITC) to asses the thermodynamics of binding of human serum albumin (HSA) to nanoparticles in the size range 70−700 nm with five different degrees of hydrophobicity. The study employs a series of copolymeric particles in which the monomers *N*-*iso*-propylacrylamide (NIPAM) and *N*-*tert*-butylacrylamide (BAM) comprise a total of 91% by weight and the cross-linker *N*,*N*-methylenebisacrylamide constitutes 9%. The BAM monomer has an additional $-CH_3$ group relative to NIPAM, and polymers with different hydrophobicity are obtained by varying the ratio of the two components. The NIPAM/BAM ratios used in this study range from 100:0 to 50:50, with 100:0 being the most hydrophilic particle. The monomers are water soluble, while the growing polymers undergo phase separation as the synthesis is conducted at a temperature higher than the lower critical solution temperature (LCST) of the NIPAM part of the polymers.[12] When polymerization occurs in the presence of SDS micelles, the growing polymers will enter the micelles to avoid contact with the surrounding water. The number of micelles will determine the size of the resulting nanoparticles, and the higher the surfactant concentration, the more distributed the growing polymer chains, and thus the smaller the resulting nanoparticles. At limiting SDS concentration, the particles will get fewer but larger. In this way, we obtained a series of nanoparticles with defined size from 70 to 700 nm. Details about the particle synthesis can be found in Supporting Information and refs 13−15.

The protein chosen for this study, HSA, is the most abundant serum protein and is known to bind several small hydrophobic endogenous and exogenous ligands. The protein is often used as a blocking agent due to its high propensity to bind to various surfaces. The molecular weight of HSA is 66 kDa, and the protein has a high α-helical content and three domains. Under normal conditions in blood, unsaturated fatty acids are bound to the protein. The monounsaturated oleic acid is the most abundant ligand and appears to have seven binding sites of varying affinity on HSA.[16] For a review of ligand binding to HSA, see, for example, ref 17.

We chose to evaluate the use of ITC for protein−nanoparticle interactions because it is a straightforward method for studying association reactions and has long been used to accurately measure ligand-binding properties. One component is titrated into another component at constant pressure, and the difference in heat that needs to be added to the sample cell compared to the reference cell in order to keep the two at the same temperature is accurately monitored. From several repeat injections, a binding curve can be obtained, and the affinity, stoichiometry, and enthalpy change upon binding can be derived.

To quantify HSA binding as a function of nanoparticle characteristics, we titrated the protein into nanoparticle solutions and monitored the heat response using ITC. The protein was dissolved to 40 μM in 10 mM Hepes/NaOH buffer (pH 7.5) with 150 mM NaCl and 1 mM EDTA. The protein concentration was determined by amino acid analysis after acid hydrolysis (purchased from BMC, Uppsala). An extinction coefficient was derived and was used for concentration determinations of subsequent protein stock solutions. The particles were dissolved to a concentration of 1 mg/mL in the Hepes buffer on ice. This yields molar concentrations of 9.3, 1.84, 0.4, 0.05, and 0.0093 nM for the 70, 120, 200, 400, and 700 nm particles, respectively. The pH of the protein solution was adjusted to match the pH of the particle solution (pH 7.5). Particle and protein solutions were equilibrated to 5 °C and degassed prior to each titration. A first 1 μL injection was followed by aliquots of 5 μL of the protein solution that were titrated into the nanoparticle solution with a total number of 60 injections to obtain complete binding curves in all cases. From the known concentrations of protein and particles, the stoichiometry, affinity, and enthalpy changes upon binding were derived from a simple fit to the data of a one-site binding model using the software ORIGIN (Microcal, Northhampton, MA). In order to determine the heat of dilution, HSA at the same concentration as in the particle-binding experiments was titrated into buffer. In this blank titration, the first few injections had the shape of a binding curve although at low signal. This may be due to dissociation of protein dimers present at the high protein concentration in the syringe. The obtained parameter values from the fitting process were only marginally changed with the subtraction of the blank titration, and the reported values are without subtraction as the total concentration of HSA in the blank titration does not correspond to the free concentration of HSA obtained in the particle-binding experiments. However, we show the blank curve for comparison.

We show here that ITC can provide very useful data with high signal-to-noise ratio for HSA binding to several of the tested nanoparticles. Raw data and fitted curves for HSA titrated into nanoparticles of different hydrophobicity are shown in Figure 1. As can be seen, the association reaction is exothermic for all levels of nanoparticle hydrophobicity. Strikingly, a much larger number of injections are needed to reach saturation for the more hydrophobic particles compared to the more hydrophilic ones, implying a higher surface coverage for the more hydrophobic particles. Furthermore, the signal for the 75:25, 85:15, or 100:0 NIPAM/

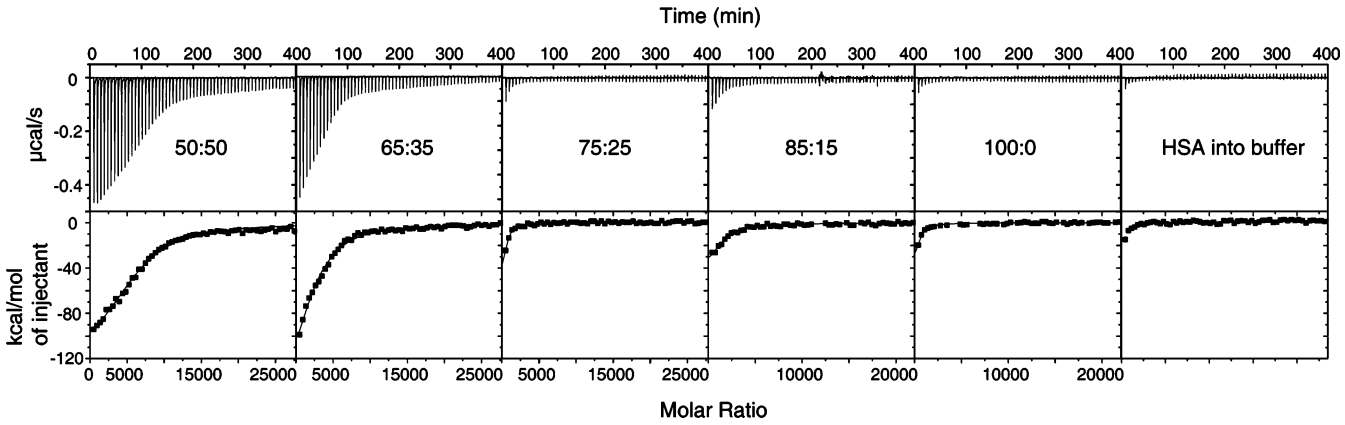

Figure 1. ITC data for titration of HSA into solutions of 200 nm polymeric nanoparticles of varying hydrophobicity in 10 mM Hepes/NaOH, 0.15 M NaCl, 1 mM EDTA, pH 7.5, 5 °C. The particle concentration in the cell (1.4 mL) was 0.4 nM, and the protein concentration in the syringe was 40 μM. The upper panels show raw data, and the bottom panels show integrated heats in each injection together with a fit using a one-site binding model. The 50:50 NIPAM/BAM particles are the most hydrophobic and 100:0 are the most hydrophilic. The last panel shows protein titrated into buffer for comparison.

Table 1. Stoichiometries, Affinities (K_A), and Enthalpy Changes upon Binding when HSA was Titrated into Different Particles Solutions at 5 °C[a]

size (nm)	NIPAM/BAM	stochiometry	degree of coverage	K_A (10^6 M^{-1})	ΔH (kJ/mol)	ΔS (kJ/mol·K)	n
70	50:50	320 ± 36	0.52 ± 0.06	1.20 ± 0.02	−595 ± 54	−1.95 ± 0.23	4
	65:35	201 ± 91	0.32 ± 0.15	1.22 ± 0.82	−297 ± 79	−3.27 ± 2.34	3
	85:15	65 ± 20	0.11 ± 0.03	6.27 ± 2.32	−104 ± 53	−0.35 ± 0.04	4
120	50:50	2570 ± 440	1.50 ± 0.14	0.78 ± 0.05	−828 ± 425	−3.24 ± 1.84	3
	65:35	414 ± 258	0.24 ± 0.15	0.71 ± 0.21	−774 ± 238	−4.07 ± 2.61	6
200	50:50	5932 ± 1154	1.28 ± 0.25	1.71 ± 0.06	−473 ± 79	−1.27 ± 0.79	4
	65:35	4264 ± 1016	0.92 ± 0.22	1.60 ± 0.70	−473 ± 58	−1.93 ± 0.64	3
	75:25	693 ± 333	0.15 ± 0.08	2.33 ± 1.06	−186 ± 27	−3.11 ± 3.77	3
	85:15	1094 ± 469	0.24 ± 0.15	2.01 ± 0.99	−190 ± 50	−0.85 ± 0.43	3
	100:0	246 ± 9	0.05 ± 0.01	3.88 ± 0.06	−280 ± 138	−0.88 ± 0.70	2
400	50:50	16794 ± 1850	0.98 ± 0.11	3.70 ± 0.13	−642 ± 57	−2.04 ± 0.26	3
	65:35	1661 ± 84	0.10 ± 0.00	4.02 ± 3.08	−798 ± 157	−4.01 ± 1.16	3
700	50:50	39676 ± 23848	0.76 ± 0.46	2.03 ± 1.08	−695 ± 122	−6.62 ± 7.09	3

[a] Weighted average and standard deviations are from n measurements. The entropy change was calculated from $\Delta H - T\Delta S = -RT\ln K_A$.

BAM particles is only slightly higher than in the blank titration, indicating that adsorption to these particles occurs with a smaller enthalpy change. The affinity does not vary drastically over the hydrophobicity range, but a small trend toward higher affinity for the more hydrophilic particles is observed. The enthalpy change is negative in all cases but appears to be more negative for the most hydrophobic particles. The stoichiometries, affinities, and enthalpy changes upon binding are summarized in Table 1 for the different nanoparticle compositions and sizes.

The degree of surface coverage is an important parameter that tells whether a sparse or a dense layer of protein is adsorbed, or whether multiple layers form on the particles. To calculate the maximum number of HSA molecules adsorbed to the nanoparticles, a minimal cross-section area was estimated by analyzing the folded structure of HSA in MOLMOL.[18] The surface area of the particles at half a protein diameter above the particle was calculated and divided by the protein cross-sectional area to achieve the theoretical numbers at 100% coverage. These are 620, 1710, 4650, 17 140, and 51 900 HSA molecules for the 70, 120,

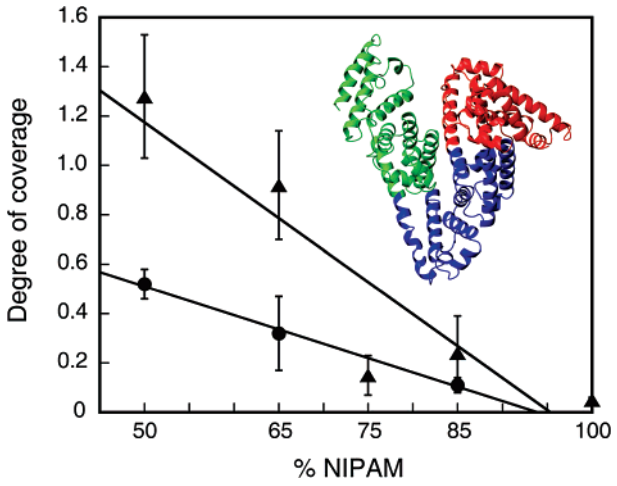

Figure 2. The degree of saturation (calculated from the ratio of fitted stoichiometries and theoretical surface coverage) for the different hydrophobicities of 70 (●) and 200 nm (▲) particles. Inset: the structure of HSA (PDB 1a06) with the three domains colored in red, blue, and green.

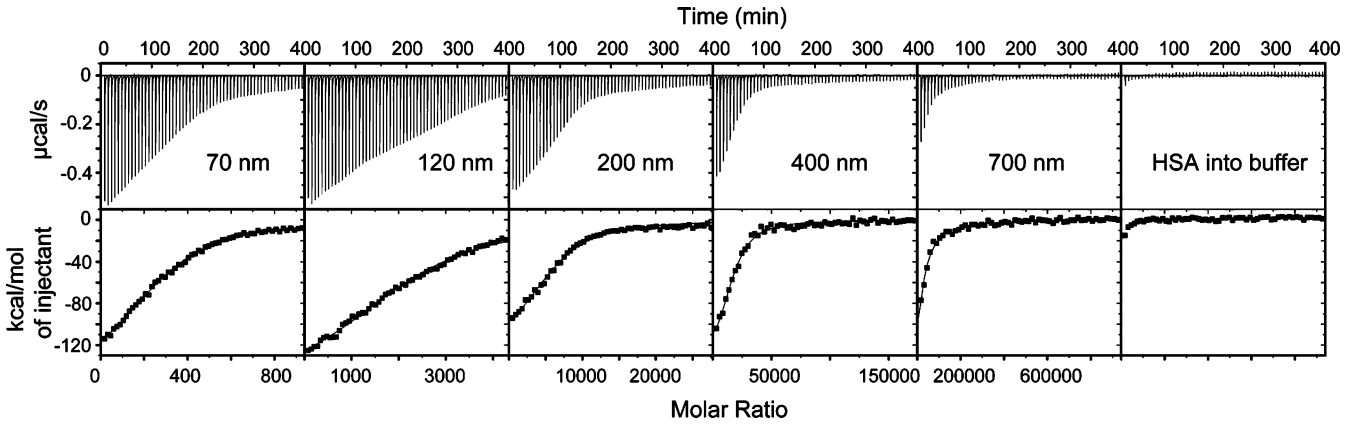

Figure 3. ITC data at 5 °C for titration of HSA into polymeric nanoparticles with 50:50 NIPAM/BAM ratio of varying size. The particle concentration in the cell (1.4 mL) was 1 mg/mL corresponding to 9.3, 1.84, 0.4, 0.05, and 0.0093 nM for the 70, 120, 200, 400, and 700 nm particles, respectively. The protein concentration in the syringe was 40 μM. The upper panels show raw data, and the bottom panels show integrated heats together with a fit using a one-site binding model. The last panel shows protein titrated into buffer for comparison.

200, 400, and 700 nm particles, respectively. From these numbers, and the obtained stoichiometries, the degree of surface coverage was calculated for each particle tested. The surface coverage for the 70 and 200 nm particles as a function of hydrophobicity is shown in Figure 2, and the values for all particles are given in Table 1. The surface coverage is clearly strongly dependent on the particle hydrophobicity, and we find the same trend for the two particle sizes. The most hydrophobic particles bind considerably more HSA than the more hydrophilic ones. For particles with 25% BAM and below, very little HSA binding is observed. This is in agreement with a recent study in which bovine serum albumin had preferential binding to CH_3 compared to OH-terminated surfaces.[19] Additionally, we have shown that the amount of CH_3 groups at the surface increases with increasing BAM content, at the expense of the more polarizable −NH groups.[20] Even though a surface coverage of 91% would be expected for hexagonal dense packing of ideal spheres in a monolayer, the numbers that we obtain are around or slightly above 100% and most likely reflect a single layer as the particles are somewhat expanded at 5 °C. The important finding is the clear effect of particle hydrophobicity in determining the amount and nature of nanoparticle surface binding.

To investigate the influence of nanoparticle size (curvature) on protein adsorption, titration experiments were performed for 50:50 NIPAM/BAM particles with varying size from 70 to 700 nm (Figure 3). The results of these experiments indicate a surface coverage of 52 ± 6% for the smallest (70 nm) and around or slightly above 100% for the 120−400 nm particles (Figure 4). The 700 nm particles have the same surface coverage as the 200−400 nm particles within experimental error. The very low total surface area available on the 700 nm particles offers a technical challenge, yielding larger errors than for the smaller particles. The smaller the particles, the larger the surface area presented at the same weight-per-volume concentration, and thus the better the precision in the ITC measurements. The striking result here is the lower degree of surface coverage observed for the smaller particles, which suggests that a higher degree of surface curvature interferes with binding. In theory, there

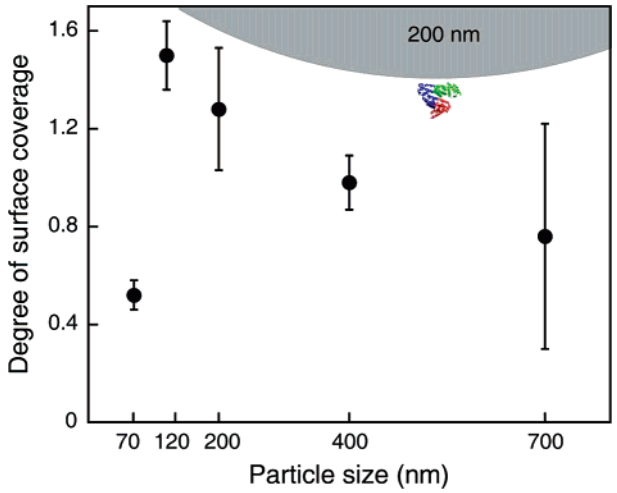

Figure 4. The degree of saturation (calculated from the fitted stoichiometries and the theoretical surface coverage) for 50:50 NIPAM/BAM particles versus particle size. Inset: size comparison of albumin and a 200 nm particle.

should be a size limit above which the binding properties are independent of curvature and approach those of a "flat" surface, and this limit seems to occur with particles of between 70 and 120 nm diameter. The circumference of a 70 nm particle can hold 31 HSA molecules of 8 nm diameter, while 53 proteins fit in a circle around the 120 nm particle. Thus, for the 70 nm particle, some strain may be expected and it may not be possible to fit in all proteins around the poles, while one would expect the coverage to approach a constant value for all sizes ≥120 nm, as observed. Alternatively, it is possible that on flat surfaces, or surfaces with low curvature, the adsorbed protein molecules form a two-dimensional ordered structure reinforced by repetitive "crystal contacts" between proteins. At higher curvature, proteins are spatially deflected from their neighbors and these crystal contacts cannot form.

For nanoparticles with a diameter of 120 nm or larger, our results seem to imply that the protein adsorbs in a dense monolayer. However, it may be that there is an enthalpy change upon binding of a first protein layer, and that binding

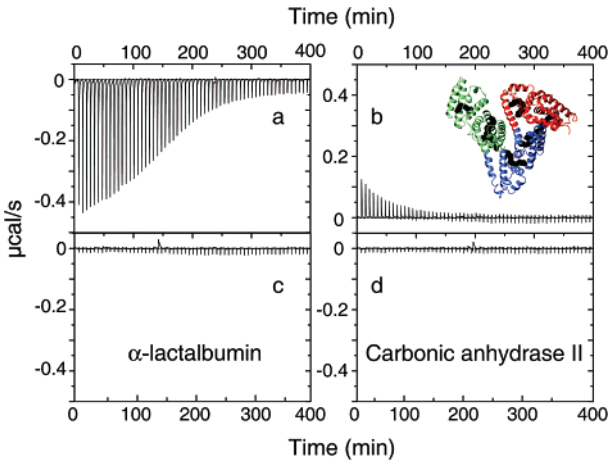

Figure 5. Raw ITC data for different proteins titrated into a 9.3 nM solution of 70 nm 50:50 particles: (a) HSA, (b) HSA in complex with oleic acid, (c) α-lactalbumin, and (d) human carbonic anhydrase II. All panels are plotted on the same scale, and the proteins are injected at approximately the same molar concentrations. In (b), the scale has the same magnitude but with endothermic heats instead of exothermic. Panel b inset: structure of HSA with oleic acid bound (PDB 1gni).

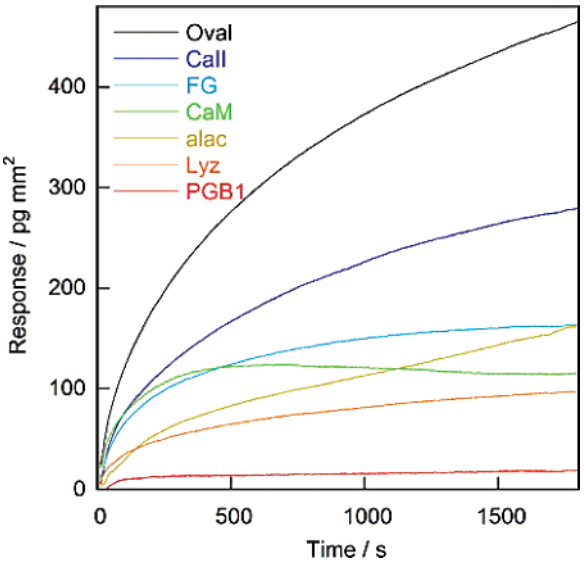

Figure 6. SPR data for ovalbumin (black), carbonic anhydrase II (blue), fibrinogen (light blue), calmodulin (green), α-lactalbumin (brown), lysozyme (orange), and the protein G B1 domain (red) injected over 70 nm 50:50 NIPAM/BAM particles linked via a thiol group to gold. Each protein was dissolved at 5−20 μM in 10 mM Hepes/KOH, 0.15 M NaCl, pH 7.4, with 3 mM EDTA and 0.005 Tween20. The same buffer was used as the running buffer.

of additional layers occurs with only changes in entropy and is thus not observable by ITC. Multilayer adsorption is usually identified by detectable steps as the layers become completed.[21] For example, in a previous calorimetry study of lysozyme, the adsorption isotherm showed a stepwise pattern, and the authors suggested that the different steps resulted from distinct conformational states of lysozyme upon adsorption to the surface.[22] We do not identify such steps, but again, it could be that it is only the first layer of HSA that shows an enthalpy change upon binding. In a recent study of statherin adsorption to hydroxyapatite crystals, the authors argued that there were two types of adsorption sites on the crystal and that only one of the sites gave rise to a change in enthalpy.[23]

Due to the limited solubility of the nanoparticles in water and buffers at room temperature (i.e., above the LCST of many of the copolymer particles), the majority of the experiments were performed at 5 °C where the solubility is higher and particle concentrations sufficient for the ITC experiments could be obtained. Control experiments were performed with lower particle and protein concentrations at 5 °C intervals from 5 to 40 °C. The results at 5−15 °C yield similar stoichiometries, and the enthalpy change is the same, within experimental error. For 20−40 °C, the same exothermic process is observed, although the stoichiometry appears to be lower. However, the quality of data is much poorer due to the reduced signal-to-noise ratio at low particle and protein concentrations and due to the onset of particle aggregation.

Oleic acid is the normal endogenous ligand for HSA, and thus, adsorption of the HSA−oleic acid complex to the nanoparticles was investigated. The observed heats are now drastically changed, and the binding seems to be endothermic (Figure 5). This change might be due to a change in the binding mode of the protein, or alternatively that the oleic acid first has to dissociate from the protein before the protein can adsorb to the nanoparticles, resulting in an uptake of heat. Binding of oleic acid to HSA is an exothermic process, and conversely, if the fatty acid is released, heat is taken up. The overall process of fatty acid release and protein adsorption to the particles might be entropically favored but occurs to a much lesser extent than in the absence of the competing ligand. Another suggestion is that the endothermic process is caused by binding of oleic acid to the particles. This process is found to be endothermic (data not shown) and may be greater in magnitude compared to HSA adsorption to the particle, making the overall signal endothermic.

Particle binding of several other proteins, α-lactalbumin, calmodulin, lysozyme, fibrinogen, protein G B1 (PGB1) domain, ovalbumin, and human carbonic anhydrase II, was studied, but no signals were observed by ITC (data for two of these proteins are shown in Figure 5). The reason for this lack of signal could be that adsorption occurs without an enthalpy change (that is, the binding is entirely entropy driven due to the release of water), or that these proteins may not bind to the particles. Adsorption of the proteins to the particles was therefore investigated by surface plasmon resonance technology. In these experiments, the same proteins were injected one-by-one over 70 nm 50:50 particles that had been linked via a thiol group to gold.[10] For the PGB1 domain, no significant association was detected, whereas α-lactalbumin, calmodulin, lysozyme, fibrinogen, ovalbumin, and human carbonic anhydrase II were all found to interact with the 70 nm 50:50 particles (Figure 6). Thus we can conclude that PGB1 associates weakly or not at all with the particles, while for the majority of the proteins tested, association with the particles is an entropy-driven process. This is a remarkable phenomenon from a fundamental point of view and highlights the point that one needs to be careful to use several complementary methods in such studies in

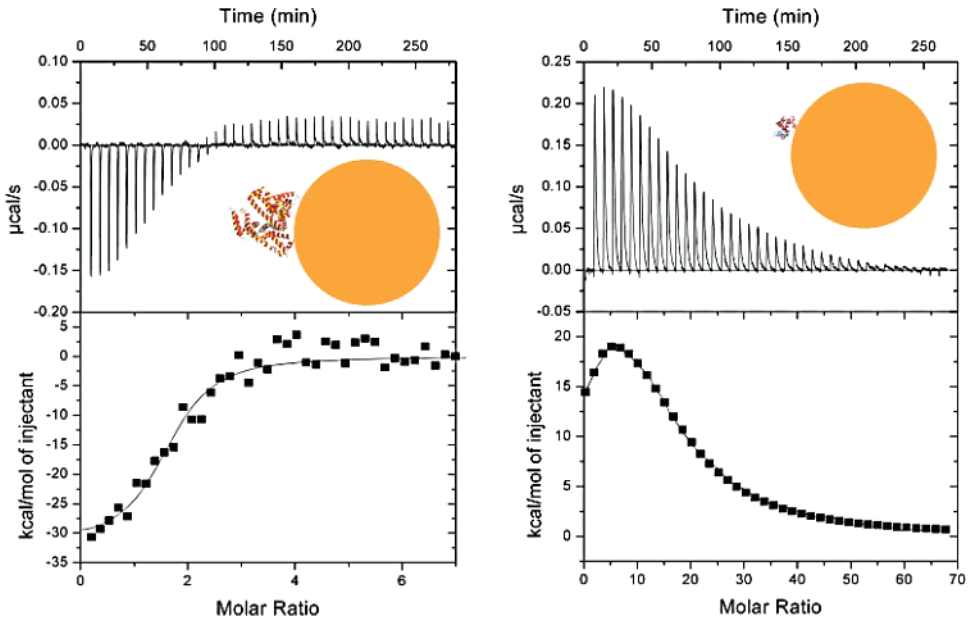

Figure 7. ITC data at 5 °C for titration of protein into solutions of quantum dots (16 nm) in 10 mM Hepes/NaOH, 0.15 M NaCl, 1 mM EDTA, pH 7.5, 25 °C. Left panel shows HSA (38 μM) titrated into an 800 nM quantum dot solution. The right panel shows α-lactalbumin (230 μM) titrated into a 500 nM solution of quantum dots. The upper panels show raw data, and the bottom panels show integrated heats in each injection together with the best fit. The insets show a size comparison of the particle and protein.

order to fully understand and characterize the nature of the adsorbed protein layer that deposits on nanoparticles in physiological environments.

From thermodynamic data, it is always tempting to discuss the underlying interactions involved in the binding event; however, it is never straightforward to rationalize the driving forces for binding. Commonly, binding due to the hydrophobic effect is thought to result in a large entropy increase and positive enthalpy change. However, the hydrophobic effect has a pronounced temperature dependence, with an optimum around room temperature where the enthalpy change upon binding should also be largest. HSA is considered to be a very hydrophobic protein, and hence, it is reasonable to think that hydrophobic interactions are responsible for the adsorption of HSA to the hydrophobic nanoparticles. The temperature dependence of the hydrophobic effect predicts that ΔH and ΔS should decrease with temperature. In our measurements at different temperatures, we see a slight negative slope for ΔH versus temperature (negative ΔC_p) which points to the hydrophobic effect as a driving force. However, due to the low signal for these experiments, the enthalpy change is accompanied by large errors. An alternative hypothesis is that there are specific interactions between the protein and the side groups presented on the particle surfaces resulting in heat release. To test this alternative, protein was titrated into linear (non-cross-linked) 50:50 NIPAM/BAM copolymer at 0.33 mg/mL, yielding approximately 4.5 times as many exposed side groups as for a 1 mg/mL 70 nm particle solution. A small enthalpy change was observed, but the signal for the polymer solution was about 20% lower compared to the signal for the particle solution, indicating that the presented particle surface is a major factor driving the interaction between the protein and the nanoparticles.

The distinct exothermic nature of HSA adsorption to the copolymer particles is not a unique feature for this protein−particle combination. Preliminary investigations of protein binding to hydrophilic polymer-coated quantum dots[24] of 16 nm diameter indicate an exothermic process for HSA also in the case of these metallic particles that are considerably smaller than the copolymer particles (Figure 7). For α-lactalbumin binding to the same quantum dots, we observe a biphasic titration that is dominated by an endothermic process (Figure 7), illustrating that ITC can also be used to quantify protein adsorption to nanoparticles when ΔH for the process is positive. For both proteins, the degree of surface coverage appears to be on the order of a few percent, suggesting that a size series of quantum dots may provide further insights into the role of particle curvature.

The NIPAM/BAM nanoparticle system offers many advantages in physical and biological studies of nanoparticle function. The particles are nontoxic[14,25] and can be modified in terms of size and surface chemistry, not only with regard to hydrophobicity. Using an extended set of side groups, one may, for example, build in various degrees of positive or negative charge density. The role of adsorbed proteins can be evaluated by comparing cellular effects of nanoparticles alone, protein alone, and particles coated with protein, as a function of particle size and surface characteristics. ITC is a nonperturbing method and can be used to verify that the particles are saturated with protein before they are used in these studies. An advantage of the ITC method is that no modifications are needed in order to study nanoparticle−protein interactions, and the technique could easily become a standard tool for quantitative measurements. Additionally, in the case of particle-bound proteins with enzymatic activity, ITC could be used to derive the fractions of bound and free protein to interpret studies of enzymatic functionality and

quantify the activity reduction or enhancement in the presence of the nanoparticles.

In conclusion, nanoparticles typically bind proteins and exhibit different binding characteristics depending on their (apparent) hydrophobicity and radius of curvature. ITC is a straightforward method for measuring this adsorption in a quantitative manner. In particular, it can be used to study specific microscopic effects driving adsorption to give accurate degrees of adsorption and to complement more qualitative or structural methods.

Acknowledgment. This work was supported by the EU Consortium NanoInteract (K.A.D., I.L., S.Linse), Science Foundation Ireland (S.Linse, Walton Fellow; and K.A.D., I.L., RFP-Spatio-Temporal Aspects of NanoParticle interaction with cells), and the Swedish Research Council, VR (S.Linse). The supply of quantum dots by W. Parak, Ludwig Maximilians University, München, is gratefully acknowledged.

Supporting Information Available: Details of particle synthesis, protein purification, and ITC data analysis. This material is available free of charge via the Internet at http://pubs.acs.org.

References

(1) Royal Society of Chemistry and Royal Academy of Engineering. Report 2005. Nanoscience and Nanotechnologies: Opportunities and uncertainties.
(2) Rogers, L. In *The Sunday Times*, July 17th, 2005.
(3) Lynch, I.; Dawson, K. A.; Linse, S. *Sci. STKE* **2006**, *2006* (327), pe14-.
(4) Lundqvist, M.; Sethson, I.; Jonsson, B. H. *Langmuir* **2004**, *20* (24), 10639−10647.
(5) Roach, P.; Farrar, D.; Perry, C. C. *J. Am. Chem. Soc.* **2006**, *128* (12), 3939−3945.
(6) Lundqvist, M.; Sethson, I.; Jonsson, B. H. *Langmuir* **2005**, *21* (13), 5974−5979.
(7) Inoue, K. I.; Takano, H.; Yanagisawa, R.; Hirano, S.; Sakurai, M.; Shimada, A.; Yoshikawa, T. *Environ. Health Perspect.* **2006**, *114* (9), 1325−1330.
(8) Sayes, C. M.; Wahi, R.; Kurian, P. A.; Liu, Y. P.; West, J. L.; Ausman, K. D.; Warheit, D. B.; Colvin, V. L. *Toxicol. Sci.* **2006**, *92* (1), 174−185.
(9) Colvin, V. L. *Nat. Biotechnol.* **2003**, *21* (10), 1166−1170.
(10) Cedervall, T.; Lynch, I.; Lindman, S.; Berggard, T.; Thulin, E.; Nilsson, H.; Dawson, K. A.; Linse, S. *Proc. Natl. Acad. Sci. U.S.A.* **2007**, *104* (7), 2050−2055.
(11) Cedervall, T.; Lynch, I.; Foy, M.; Berggård, T.; Donnelly, S. C.; Cagney, G.; Linse, S.; Dawson, K. A. Submitted.
(12) Schild, H. G. *Prog. Polym. Sci.* **1992**, *17* (2), 163−249.
(13) Lynch, I.; Dawson, K. A. *J. Phys. Chem. B* **2004**, *108* (30), 10893−10898.
(14) Lynch, I.; Miller, I.; Gallagher, W. M.; Dawson, K. A. *J. Phys. Chem. B* **2006**, *110* (30), 14581−14589.
(15) McPhee, W.; Tam, K. C.; Pelton, R. *J. Colloid Interface Sci.* **1993**, *156* (1), 24−30.
(16) Petitpas, I.; Grune, T.; Bhattacharya, A. A.; Curry, S. *J. Mol. Biol.* **2001**, *314* (5), 955−960.
(17) Kragh-Hansen, U.; Chuang, V. T. G.; Otagiri, M. *Biol. Pharm. Bull.* **2002**, *25* (6), 695−704.
(18) Koradi, R.; Billeter, M.; Wüthrich, K. *J. Mol. Graphics* **1996**, *14*, 51−55.
(19) Roach, P.; Farrar, D.; Perry, C. C. *J. Am. Chem. Soc.* **2005**, *127* (22), 8168−8173.
(20) Lynch, I.; Blute, I. A.; Zhmud, B.; MacArtain, P.; Tosetto, M.; Allen, L. T.; Byrne, H. J.; Farrell, G. F.; Keenan, A. K.; Gallagher, W. M.; Dawson, K. A. *Chem. Mater.* **2005**, *17* (15), 3889−3898.
(21) Norde, W. *Adv. Colloid Interface Sci.* **1986**, *25* (4), 267−340.
(22) Lee, V. A.; Craig, R. G.; Filisko, F. E.; Zand, R. *J. Colloid Interface Sci.* **2005**, *288* (1), 6−13.
(23) Goobes, R.; Goobes, G.; Campbell, C. T.; Stayton, P. S. *Biochemistry* **2006**, *45* (17), 5576−5586.
(24) Liedl, T.; Keller, S.; Simmel, F. C.; Radler, J. O.; Parak, W. J. *Small* **2005**, *1* (10), 997−1003.
(25) Allen, L. T.; Fox, E. J.; Blute, I.; Kelly, Z. D.; Rochev, Y.; Keenan, A. K.; Dawson, K. A.; Gallagher, W. M. *Proc. Natl. Acad. Sci. U.S.A.* **2003**, *100*, 6331−6336.

NL062743+